

The stability and reactivity of activated acryloylcarbamates as reagents for the synthesis of *N*-1 substituted thymine and uracil – an NMR and DFT study

Radek Pohl^a, Lubomír Rulíšek^a and Dominik Rejman^{a*}



The mechanism of the decomposition of acryloylcarbamates **7a–b** yielding highly reactive isocyanates **3a–b** was proposed based on NMR measurements and quantum chemical calculations. A good agreement between the experimental kinetic data and DFT calculations allowed us to demonstrate that the stability of **7a–d** depends on the presence of methyl in the acryloyl moiety and the position of the nitro group in the nitrophenolic part of the molecule. Furthermore, the reactivity of **7a–d** with weakly nucleophilic and sterically hindered 2,4,6-tri-*tert*-butylaniline was explored by ¹H NMR demonstrating the usefulness of reagents **7a–d** offering access to a variety of 1-*N*-substituted uracils and thymines with potentially interesting biological properties. Copyright © 2010 John Wiley & Sons, Ltd. Supporting information may be found in the online version of this paper.

Keywords: DFT; mechanism; NMR; nucleosidation; thymine; uracil

INTRODUCTION

Many biologically active compounds belong to the class of nucleosides and nucleotides analogues, which play an important role in anticancer therapy^[1,2] or act as antiviral compounds.^[3] Specific examples also involve carbocyclic nucleosides^[4,5] (Carbovir[®]) and acyclic phosphonate nucleotides^[6] (Viread, Cidofovir, Tenofovir, Hepsera), which represent biologically important compounds in which the nucleobase is not connected via a glycosidic bond.

From a synthetic point of view, a crucial step in their preparation is the attachment of the nucleobase – the nucleosidation reaction. The most common synthetic routes to purine nucleoside analogues are represented by direct alkylation of the appropriate nucleobases (adenine, 6-chloropurine or 2-amino-6-chloropurine) with the halo, tosyloxy or mesyloxy derivatives in dipolar aprotic solvents (DMF, DMSO) using cesium carbonate as a base.^[7–9] Alternatively, Mitsunobu reaction of 6-chloropurine or 2-amino-6-chloropurine with appropriate hydroxyderivative can be used.^[8,10,11] Recently, *N*-bis-Boc-protected^[6] adenine was successfully used as a substrate for the Mitsunobu reaction during the synthesis of neplanocin A.^[12] However, all of these methods for the introduction of pyrimidine nucleobases (uracil, thymine and cytosine) suffer from both low regioselectivity and low yield of the 1-*N*-substituted product. The direct alkylation of nucleobases is usually accompanied by a competing elimination reaction, which further decreases the yield of the desired product.^[8,9] Some improvement (both in regioselectivity and overall yield) can be obtained through the use of 2,4-dimethoxy-pyrimidine or 2,4-dimethoxy-6-methylpyrimidine for the alkylation instead of uracil or thymine, respectively.^[13–15] As an

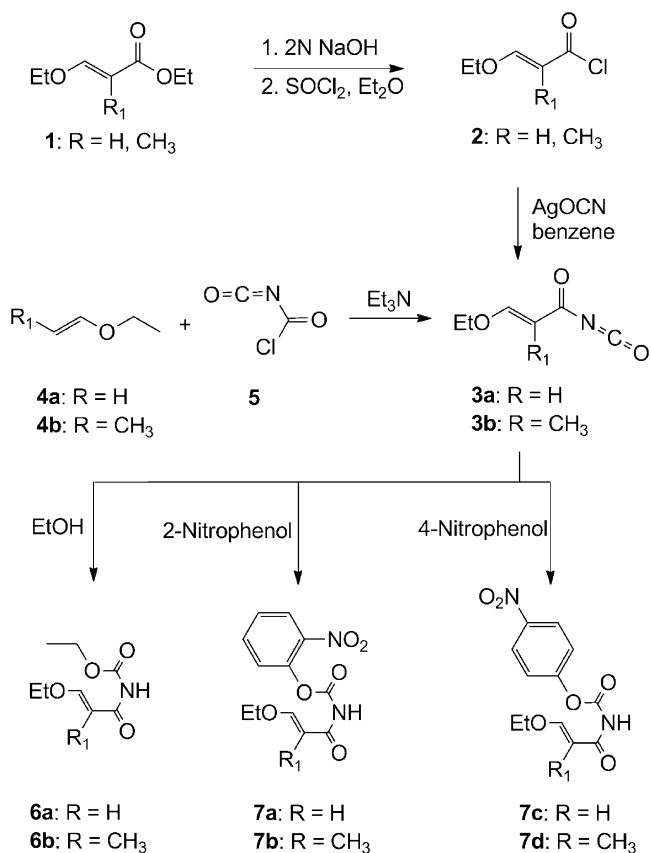
alternative approach to the pyrimidine nucleoside analogues (e.g. carbocyclic nucleosides), a synthesis of 1-*N*-substituted nucleobases starting from a primary amine and isocyanates **3a–b** or carbamates **6a–b** were described fifty years ago by Shaw and Warrener.^[16,17] The key isocyanates **3a–b**, accessible through two independent routes^[18,19] (Scheme 1), were used as intermediates for the synthesis of carbamates **6a–b** described by Hřebabecký *et al.*^[20]

Isocyanates **3a–b** are an unusually moisture-sensitive species and also very reactive compounds, capable of forming carbamates with free hydroxy groups.^[21] Therefore, the reaction is usually carried out either with the appropriately protected substrate or without protection at low temperature (<–20 °C). This property seems to be the main factor responsible for the varying yield of the reported uracil and thymine derivatives (usually ~20–80%, in most cases <60%) found in the literature.^[22–33] The formation of uracil and thymine rings is a two-stage reaction consisting of the aminolysis of carbamates **6a–b** or the addition of amine to isocyanates **3a–b** followed by a cyclisation of the acryloylureas **9** formed (Scheme 2).^[34]

Till date, there has not been any general, high-yield method available for the attachment of uracil and thymine moieties to

* Correspondence to: D. Rejman, Institute of Organic Chemistry and Biochemistry AS CR, v.v.i., Flemingovo nám. 2, 166 10 Prague 6, Czech Republic. E-mail: rejman@uochb.cas.cz

^a R. Pohl, L. Rulíšek, D. Rejman
Institute of Organic Chemistry and Biochemistry AS CR, v.v.i., Flemingovo nám. 2, 166 10 Prague 6, Czech Republic



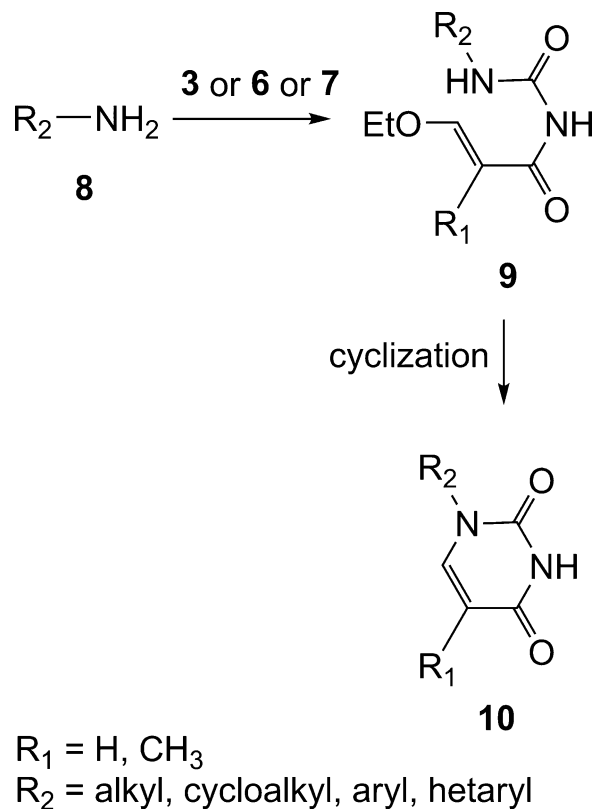
Scheme 1. The reagents for the preparation of 1-*N*-substituted pyrimidine nucleobases

sterically hindered secondary, tertiary or even aromatic carbon atoms.

It was the extreme reactivity and moisture sensitivity of isocyanates **3** on the one hand and the low yields of **9** obtained using carbamates **6** on the other that prompted us to develop more advantageous reagents **7**, which proved to be reactive enough with a variety of amines. Moreover, they can be stored for longer time (several months in refrigerator), which enabled us to use them in modular syntheses of uracils and thymines **10**.^[35] The synthesis of the reagents **7a–d** followed the procedure described for **6**,^[20] in whose last step of the 'one-pot' synthesis, a 2- or 4-nitrophenol solution in dioxane was added instead of ethanol.

The reagents **7a–d** were tested in reactions with a wide variety of amines (including those bonded to secondary, tertiary and aromatic systems), giving consistently high yields of corresponding 1,3-disubstituted urea derivatives. The desired uracil and thymine derivatives were obtained by the cyclisation of the urea intermediates using Dowex 50 in H⁺ form, providing again very high yields.^[35]

In this work, we wish to address an unprecedented decomposition of the reagent **7b** in CDCl₃ solution observed in the ¹H NMR measurements, to analyse and quantitatively characterise the reaction mechanism of the decomposition reaction. To this end, we conducted a series of NMR experiments to yield reliable kinetic data and a series of DFT calculations to provide a plausible mechanistic view of the studied reaction. In order to understand the reaction mechanism in detail, we have compared the experimental data with other reagents **7a**, **7c** and **7d**. We have also investigated the reaction of **7a–d** with low nucleophilic and



Scheme 2. The reaction of reagents **3**, **6** and **7** with amines and subsequent cyclisation providing 1-*N*-substituted pyrimidines

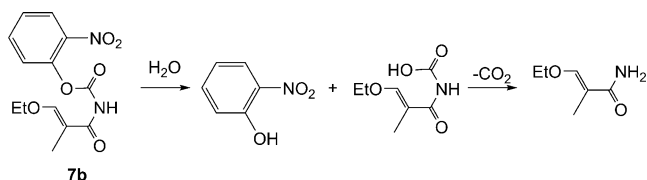
sterically hindered 2,4,6-tri-*tert*-butylaniline to ensure that decomposition of **7a–b** does not limit their synthetic usage in preparation of *N*-1 substituted thymines and uracils. These findings represent a useful and successful conjunction of theoretical and experimental efforts extending our understanding of the organic reactions pertinent to this class of compounds.

RESULTS AND DISCUSSION

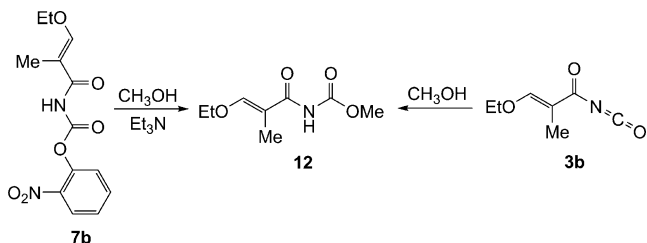
Kinetics of decomposition studied by NMR

Reagents **7a–d** were prepared according Scheme 1 and fully characterised by ¹H and ¹³C NMR, elemental analysis, IR and MS. In the course of the NMR characterisation of **7b**, we found that the reagent decomposes, yielding a complex mixture. The ¹H NMR spectrum of **7b** recorded in commercial grade CDCl₃ (refer Supporting Information) showed a mixture of at least four compounds identified as 3-ethoxy-2-methylacryloylcarbamic acid (as the product of reagent hydrolysis), 3-ethoxy-2-methylacryloylamide (i.e. the product of the decarboxylation of the former compound), 2-nitrophenol and reagent **7b** (Scheme 3).

To rule out the effect of water, which might be present in regular CDCl₃, the ¹H NMR spectra were recorded in dried CDCl₃ and a sealed NMR tube (refer Experimental section). The experiment has again shown the decomposition of compound **7b**, and the final products of decomposition were identified as acryloylisocyanate **3b** and 2-nitrophenol. Reagent **7b** was



Scheme 3. The decomposition of **7b** via hydrolysis and decarboxylation



Scheme 4. The chemical proof of **3b** structure

characterised by NMR only when a high concentration of sample and a short measurement time were applied.

To ascertain that acryloylisocyanate **3b** is the decomposition product, we allowed the decomposed mixture to react with dry methanol, yielding methyl ester **12**, i.e. the same product as that formed through the reaction of **7b** with methanol in the presence of Et_3N (Scheme 4). In addition, isocyanate **3b** was identified by IR measured in dry CHCl_3 (the characteristic band being at 2244 cm^{-1} for asymmetric stretching vibrations of the $-\text{NCO}$ group) and by ^{13}C NMR (with the characteristic chemical shift of $-\text{NCO}$ carbon at 130.47 ppm).

The rate of decomposition was estimated based on the ^1H NMR kinetic measurement in dry CDCl_3 and sealed NMR tube at $25\text{ }^\circ\text{C}$. The concentrations of starting compounds and decomposition product(s) were obtained by integration of several corresponding signals with similar relaxation times. The rate constant for the irreversible first order kinetic model was obtained from plots of the logarithm of the starting compound concentrations versus time, while rate constant for the reversible first order kinetic model was obtained from plots of the logarithm of the starting compound concentrations minus equilibrium concentration versus time and from equilibrium constant. Experimental data for decomposition of **7b** fitted irreversible reaction with first order kinetics (Table 1 and Supporting Information) with half-life ($t_{1/2}$) of about 18 min. The kinetics measurements were also

performed for the other reagents, **7a**, **7c** and **7d**, and the results have been summarised in Table 1. The decomposition of **7a** was reversible reaction with first order kinetics (Table 1 and Supporting Information), while compounds **7c** and **7d** were stable and did not decompose at all.

As arises from Table 1, the kinetic measurements demonstrate a surprisingly strong dependence on the reagents and their structure. Reagents **7c** and **7d** (possessing a nitro group in the *para* position) do not undergo any degradation. On the other hand, the derivatives with the *ortho*-nitro group in nitrophenol moiety decompose readily, with the decomposition of the **7b**-bearing methyl group in the acryloyl part of the molecule being approximately fifty times faster than the decomposition of the **7a**-lacking methyl substituent. The different stability of the reaction products reflected in the molecular structure was further explored by DFT calculations.

Reaction mechanism of decomposition. Theoretical calculations

We first optimised all 16 planar geometries for each of **7a–d**, viz. all the possible arrangements of four double or partial double bonds in the system (64 molecular geometries in total) at the DFT(PBE)/def2-SVP level with the single-point energy calculated at the DFT(B3LYP)/def2-TZVP level. The solvation effect, zero-point energy, and contribution to the enthalpy and entropy (using the ideal gas approximation) were included as well (for details, refer Experimental section). The results of this extensive conformational search are summarised in Tables S1–S5 (refer Supporting Information). As can be seen in Tables S1–S4, the calculations predict (in all cases) the most stable isomers to possess *trans*-configuration on the $-\text{C}=\text{C}-$ double bond. This fact has been corroborated experimentally by a missing NOE interaction between the Me group and the proton on the double bond for **7a–b** or by a missing NOE between the protons of the double bond for **7c–d**. At the same time we observed NOE between protons of CH_2 group from EtO and H or CH_3 on double bond in alpha position to CO.

With regard to the proposed reaction mechanism, we have also investigated the possible isomers with the proton on either of the oxygens adjacent to the central $-\text{NH}-$ group (these calculations were carried out only for the most stable isomers). The results are also listed in Tables S1–S4 (including various terms in overall Gibbs energies), and all 24 structures of **7b** (assuming an *E* configuration on the $-\text{C}=\text{C}-$ double bond) have been schematically depicted in Fig. 1.

The calculations have shown that the 2NH-ZZZ conformer is the most stable structure for the *keto*-tautomer of **7b** whereas

Table 1. The kinetics of **7a–d** degradation monitored by ^1H NMR

Degradation	Reaction	Kinetics	k (h^{-1})	$t_{1/2}$ (h)
7a	Reversible	First-order	$3.00 \times 10^{-2(a)}$	23.1
7b	Irreversible	First-order	2.32	0.30
7c	No degradation observed			
7d	No degradation observed			

^(a) $k_+ = 1.83 k_-$.

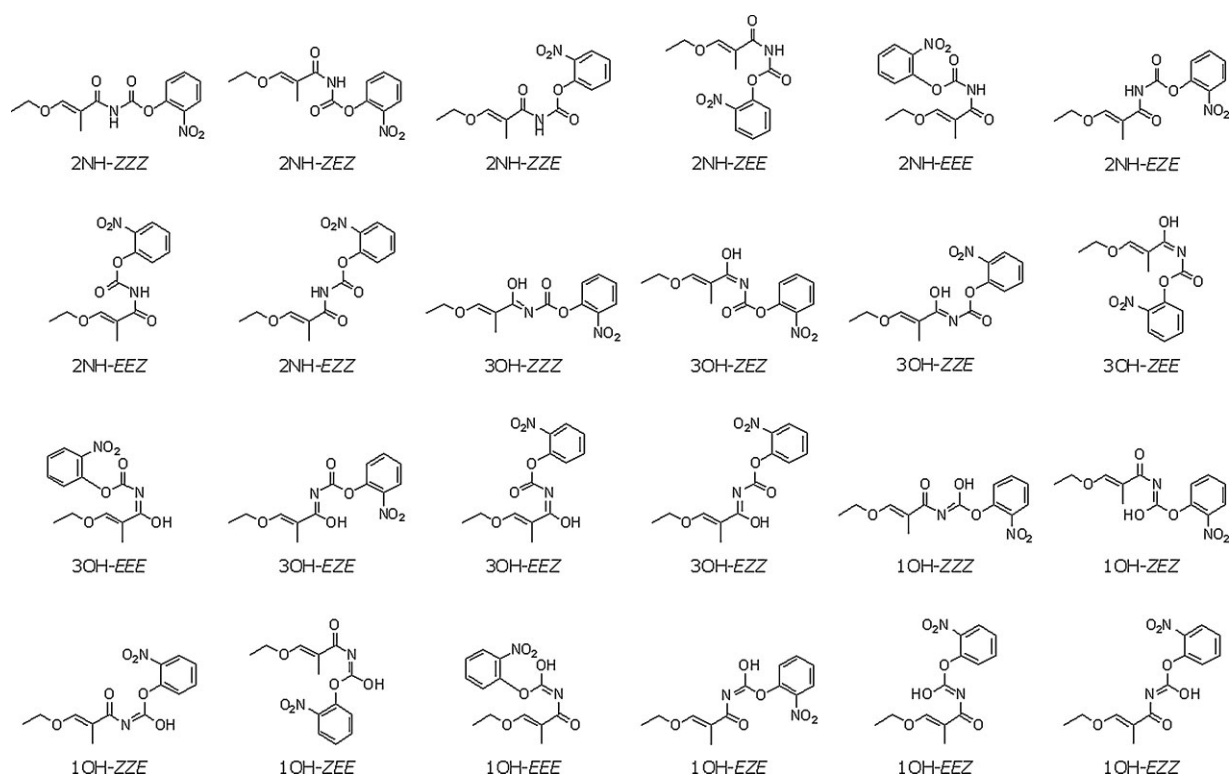


Figure 1. The planar geometries of *E*-**7b** investigated by density functional theory calculations

3OH-ZZE is the lowest energy *enol*-form of the same compound. It can be noted that 3OH-ZZE geometry is nicely preorganised to form a six-membered transition state with bifurcated hydrogen bonding.

However, a rather surprising finding is the relatively small difference in energies between all the studied isomers. Considering the planar models depicted in Fig. 1, some of the structures would have been expected to have substantial intramolecular crowding. Even for such structures (e.g. 2NH-ZEE, 2NH-EEE) the energy or free energy differences amount to only ~ 15 – 25 kJ mol $^{-1}$. This demonstrates a relatively high level of flexibility in the studied molecules (the systems avoid crowding by adopting a helical form). Thus, we had to consider several reaction pathways for the elimination reaction. The lowest saddle points and their energies are summarised in Table 2 for all studied compounds (**7a–7d**) and for the proposed reaction mechanism

of degradation shown in Scheme 5. It can be mentioned that all saddle points are characterised by a single imaginary frequency corresponding to the reactive coordinate and are therefore true transition states for the studied reactions. By small changes of the geometry in the direction of reactant and product we ascertained that it connects the desired reactant and products structures (IRC-like calculation). A more complete listing of the calculated values of activation barriers can be found in Tables S1–S4.

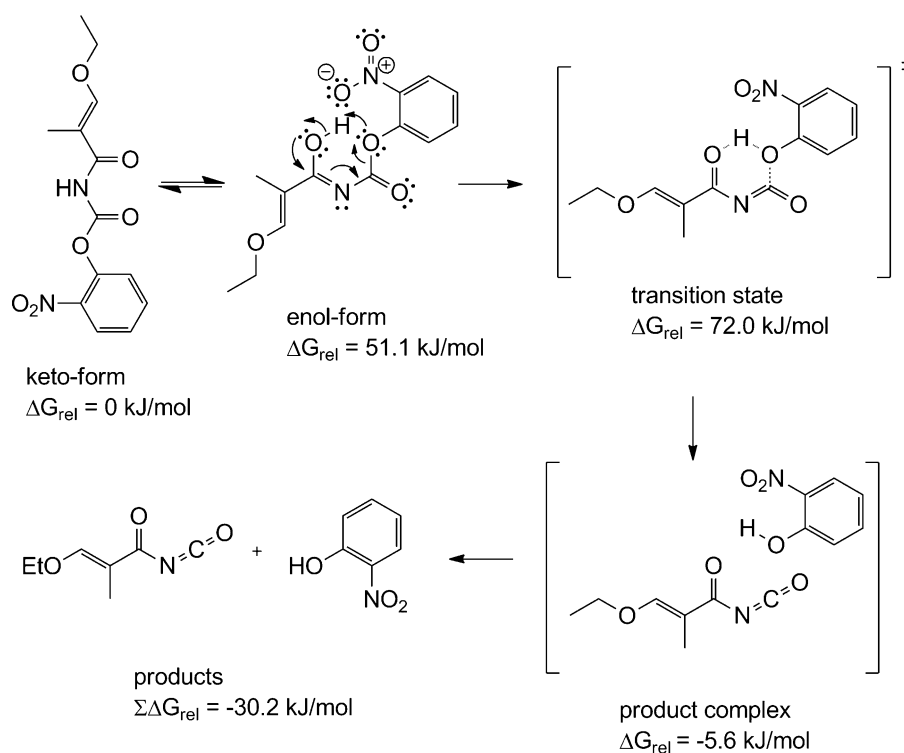
Furthermore, the reaction coordinate with the structures of all the key points on the potential energy surface is depicted in Fig. 2.

As mentioned above, the transition state is characterised by the six-membered ring arrangement and is structurally close to the *enol*-form with activation barriers of 72–88 kJ mol $^{-1}$ (Table 2). We have also investigated an alternative pathway starting from the more stable *keto*-form and involving the direct hydrogen

Table 2. The theoretical calculations of reaction free energies and activation barriers carried out using the B3LYP/def2-TZVP//RI-PBE/def2-SVP method

Degradation	ΔG_{calc} (kJ mol $^{-1}$)	$\Delta G_{\text{calc}}^{\ddagger}$ (kJ mol $^{-1}$)	k_{exp} (s $^{-1}$)	$\Delta G_{\text{exp}}^{\ddagger}$ (kJ mol $^{-1}$)
7a	–24.6	84.1	8.33×10^{-6}	102.0
7b	–30.2	72.0	6.44×10^{-4}	91.2
7c	–3.9	88.4	—	—
7d	–15.1	79.1	—	—

The solvation effects were included through COSMO calculations and the energies corrected for zero-point energies, thermal corrections to enthalpy and entropic terms (using ideal gas approximation) to obtain free energy estimates. The experimental data are shown in the right part of the table ($\Delta G_{\text{exp}}^{\ddagger}$ were calculated using Eyring equation (in SI units): $\Delta G^{\ddagger} = RT[23.76 - \ln(k/T)]$).



Scheme 5. The degradation of **7b** – a proposed mechanism

transfer from the nitrogen atom to the oxygen atom of the nitrophenol ring. The activation barrier involving a four-membered transition state was considerably higher ($\sim 160\text{--}180 \text{ kJ mol}^{-1}$, refer Tables S1, S3, S4) for the 2NH-EEZ isomer (which has the most favourable arrangement of the atoms and highest thermodynamic stability of the reactants). This clearly favours the pathways involving the six-membered transition states described above.

As arises from Table 2, the presence of the *ortho*-nitro group plays an important role in the bifurcated hydrogen bond and lowers the free enthalpy of degradation ΔG_{calc} . On the other hand, the methyl group on the —C=C— double bond lowers the free energy of activation, $\Delta G_{\text{calc}}^{\ddagger}$, likely due to the effect of hyperconjugation. The computational results are in good agreement with the experimentally calculated $\Delta G_{\text{exp}}^{\ddagger}$ computed from the rate constants using Eyring equation. Since the accurate *ab initio* determination of the *absolute rate constant* is beyond the

scope of this work (for a thorough discussion on the subject, we refer the reader to Reference [36]), we mostly want to highlight the excellent agreement in the relative difference between the two reactions (**7a**, **7b**) for which the comparison is available. $\Delta \Delta G_{\text{exp}}^{\ddagger} = 10.8 \text{ kJ mol}^{-1}$, whereas $\Delta \Delta G_{\text{calc}}^{\ddagger} = 12.1 \text{ kJ mol}^{-1}$.

NMR characterisation of the reactivity of **7a–d** towards amines

In our previous work,^[35] we showed that reagents **7a,b** react with a variety of amines, including acyclic, cyclic, and aromatic, and also amino acids. All of the reactions were completed within one hour at room temperature. Nevertheless, the reaction kinetics were not addressed in detail. Herein, the reactivity of **7a–d** with low nucleophilic and sterically hindered 2,4,6-*tert*-butylaniline is presented (Scheme 6).

The kinetic measurements were performed in dry CDCl_3 at 25°C and monitored by ^1H NMR. The concentrations of starting compounds and products were obtained by integration of several corresponding signals with similar relaxation times (for example CH_3 on double bond in **7b** and **11b**). The rate constants were obtained from plots of the logarithm of the starting compound concentrations *versus* time. Obtained data fitted first order kinetics and the results of the measurements are summarised in Table 3. The kinetic data show relatively high difference in reaction rates that might be explained by observed decomposition described above. Similar reaction rates for **7c–d** confirm the finding that these compounds do not decompose and reaction with amine can be viewed as aminolysis of 4-nitrophenyl ester. On the other hand, very fast reaction rate for **7b** corresponds with decomposition of the compound and can be therefore assumed that 2,4,6-*tert*-butylaniline reacts with isocyanate **3b** formed in course of the decomposition **7b**. The

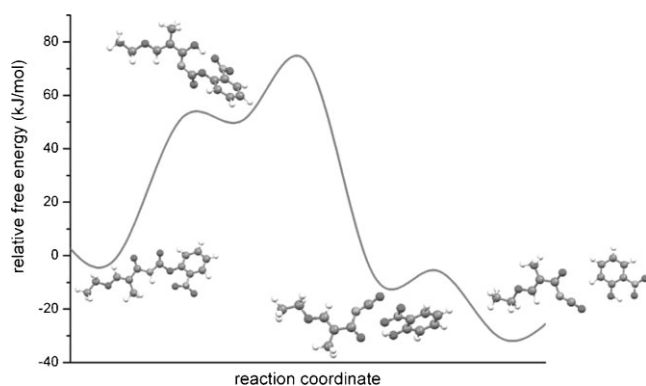
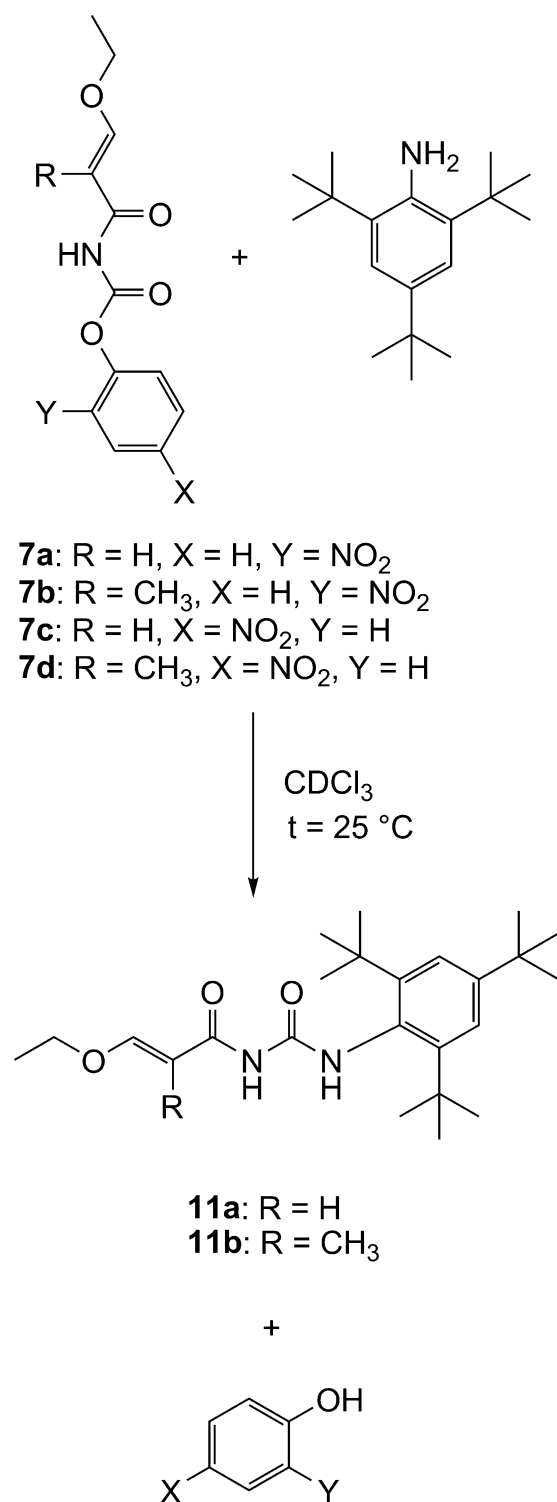


Figure 2. The reaction coordinate for the degradation of *E*-**7b**



Scheme 6. The reaction of **7a–d** with 2,4,6-tri-*tert*-butylaniline

only anomaly is reactivity of 2,4,6-tri-*tert*-butylaniline with **7a**. In this case the amine probably reacts either with acryloyl carbamate **7a** or with its decomposition product **3b** and overall reaction rate is indeed anomalous. The reaction was complete for all the studied reagents, providing substituted acryloylureas as products. The results of the kinetics show that novel reagents **7a–d** are capable of reaction even with sterically hindered

Table 3. The kinetics of the reaction of the reagents **7a–d** with 2,4,6-tri-*tert*-butylaniline in dry CDCl₃ at 25 °C.

Reagent	k (h ⁻¹)	$t_{1/2}$ (h)
7a	2.7×10^{-2}	25.7
7b	1.2	0.6
7c	7.4×10^{-2}	9.4
7d	2.7×10^{-1}	2.6

aromatic amines, which offers access to a variety of 1-*N*-substituted uracils and thymines with potentially interesting biological properties.

CONCLUSIONS

It has been shown that the studied reagents **7a–d** are highly reactive even with low-nucleophilic and sterically hindered amines and can be successfully applied for a modular synthesis of various 1-*N*-substituted uracils and thymines, which is difficult to achieve with other synthetic methods. The stability of reagents **7a–d** in dry CDCl₃ was investigated by experimental and theoretical methods. It has been proved that the decomposition of the studied molecules is strongly affected by the presence of the Me-group on the —C=C— double bond and the position of the nitro group on the phenol ring. While the former is assumed to lower the activation barrier of the reaction probably due to hyperconjugation, the latter plays a role in hydrogen bonding and influences the thermodynamics of the reaction. The experimental NMR observations are in good agreement with the results predicted by the DFT calculations, which allowed us to postulate a plausible reaction mechanism, presumably extending our understanding of the reactivity and stability of this class of compounds. It should be noted here that all the reagents are stable enough in the solid state to be stored for a long time. Moreover, the decomposition of the 2-nitrophenyl derivatives **7a** and **7b** yields an isocyanate product that could react in the same manner as the parent reagents. These compounds could be seen as an ‘instant form’ of the previously described isocyanates **3a–b**.

EXPERIMENTAL SECTION

NMR experiments

NMR spectra were acquired on a Bruker Avance 500 spectrometer (500.0 MHz for ¹H and 125.7 MHz for ¹³C) in dry CDCl₃. CDCl₃ was dried prior to use by anhydrous K₂CO₃ and distilled. The measurements were performed in an oven-dried NMR tube, which was sealed after sample preparation. The concentration of the samples was 38 and 40 mM for the degradation kinetics and kinetics of reaction with amines, respectively. All of the kinetic measurements were performed at 25 °C. Temperature calibration was done using the standard method with a MeOH sample. ¹H and ¹³C resonances were assigned based on PFG H,C-HSQC and H,C-HMBC experiments (for numbering refer Supporting Information). ¹H and ¹³C NMR of compounds **7a–d** have been already reported.^[35]

Computational details

All the density functional theory (DFT) calculations reported in the study were carried out using the Turbomole 6.0 program.^[37] The Perdew–Burke–Ernzerhof (PBE)^[38] and hybrid three-parameter Beckés^[39–42] (B3LYP) functionals were used throughout. The calculations were expedited by expanding the Coulomb integrals in an auxiliary basis set, the resolution-of-identity (RI-J) approximation.^[43,44] All the geometry optimisations were conducted using the def2-SVP basis set,^[45,46] whereas the single-point energies were recomputed in the def2-TZVP (triple-zeta valence with two polarisation functions on each atom).^[47]

To account for the solvation effects, the conductor-like screening model (COSMO) method^[45–48] was used with the dielectric constant corresponding to chloroform ($\epsilon_r = 4.9$). In order to account for dispersion, we used the DFT + D method (i.e. the DFT method with the empirical dispersion terms) available in Turbomole 6.0.^[49] The Gibbs free energy was then calculated as the sum of these contributions:

$$G = E_{\text{el}} + G_{\text{solv}} + E_{\text{ZPE}} - RT \ln(q_{\text{trans}} q_{\text{rot}} q_{\text{vib}}),$$

where E_{el} is the *in vacuo* energy of the system (at the B3LYP/def2-TZVP level and the geometry optimised at the RI-PBE/def2-SVP level), G_{solv} is the solvation free energy (at the RI-PBE/def2-SVP level), E_{ZPE} is the zero-point energy and $-RT \ln(q_{\text{trans}} q_{\text{rot}} q_{\text{vib}})$ accounts for the entropic terms and the thermal correction to the enthalpy obtained from a frequency calculation using the same method and software as for the geometry optimisation at the RI-PBE/def2-SVP level, 298 K, and 1 atm using the ideal-gas approximation.^[50]

(E)-3-Ethoxy-2-methylacryloyl isocyanate (3b)

¹H NMR (CDCl₃, 500.0 MHz): 1.36 t, 3H, $J(\text{CH}_3, \text{CH}_2) = 7.1$ (CH₃CH₂O); 1.82 d, 3H, $J(\text{CH}_3, \text{CH}) = 1.2$ (CH₃); 4.13 q, 2H, $J(\text{CH}_2, \text{CH}_3) = 7.1$ (OCH₂CH₃); 7.53 q, 1H, $J(\text{CH}, \text{CH}_3) = 1.2$ (CH=). ¹³C NMR (CDCl₃, 125.7 MHz): 8.79 (CH₃); 15.34 (CH₃CH₂O); 70.98 (OCH₂CH₃); 110.19 (C=); 130.47 (NCO); 162.82 (CH=); 165.52 (CO).

1-(2,4,6-Tri-tert-butylphenyl)-3-((E)-3-ethoxyacryloyl)urea (11a)

¹H NMR (CDCl₃, 500.0 MHz): 1.30 s, 9H ((CH₃)₃C-4'); 1.32 t, 3H, $J(\text{CH}_3, \text{CH}_2) = 7.1$ (CH₃CH₂O); 1.40 s, 18H ((CH₃)₃C-2',6'); 3.90 q, 2H, $J(\text{CH}_2, \text{CH}_3) = 7.1$ (OCH₂CH₃); 5.26 d, 1H, $J(5,6) = 12.2$ (H-5); 7.40 s, 2H, (H-3',5'); 7.72 d, 1H, $J(6,5) = 12.2$ (H-6); 8.54 bs, 1H (H-3); 10.29 bs, 1H (H-1). ¹³C NMR (CDCl₃, 125.7 MHz): 14.48 (CH₃CH₂O); 31.38 ((CH₃)₃C-4'); 31.86 ((CH₃)₃C-2',6'); 34.97 ((CH₃)₃C-4'); 36.19 ((CH₃)₃C-2',6'); 67.87 (OCH₂CH₃); 97.48 (C-5); 122.93 (C-3',5'); 129.26 (C-1'); 148.01 (C-2',6'); 149.55 (C-4'); 154.77 (C-2); 163.84 (C-6); 168.26 (C-4). HR-MS for C₂₄H₃₉N₂O₃ (M + H)⁺ calcd 403.2955, found 403.2955.

1-(2,4,6-Tri-tert-butylphenyl)-3-((E)-3-ethoxy-2-methylacryloyl)urea (11b)

¹H NMR (CDCl₃, 500.0 MHz): 1.31 s, 9H ((CH₃)₃C-4'); 1.33 t, 3H, $J(\text{CH}_3, \text{CH}_2) = 7.1$ (CH₃CH₂O); 1.42 s, 18H ((CH₃)₃C-2',6'); 1.84 d, 3H, $J(\text{CH}_3, 6) = 1.2$ (5-CH₃); 4.04 q, 2H, $J(\text{CH}_2, \text{CH}_3) = 7.1$ (OCH₂CH₃); 7.43 s, 2H, (H-3',5'); 7.58 q, 1H, $J(6, \text{CH}_3) = 1.2$ (H-6); 7.95 bs, 1H (H-3); 10.45 bs, 1H (H-1). ¹³C NMR (CDCl₃, 125.7 MHz): 8.83 (5-CH₃); 15.44 (CH₃CH₂O); 31.37 ((CH₃)₃C-4'); 31.87 ((CH₃)₃C-2',6'); 34.98 ((CH₃)₃C-4'); 36.20 ((CH₃)₃C-2',6'); 70.54 (OCH₂CH₃); 105.68 (C-5);

123.04 (C-3',5'); 129.30 (C-1'); 147.97 (C-2',6'); 149.53 (C-4'); 154.33 (C-2); 158.71 (C-6); 169.64 (C-4). HR-MS for C₂₅H₄₁N₂O₃ (M + H)⁺ calcd 417.3112, found 417.3111.

Methyl (E)-3-ethoxy-2-methylacryloylcarbamate (12)

¹H NMR (CDCl₃, 500.0 MHz): 1.33 t, 3H, $J(\text{CH}_3, \text{CH}_2) = 7.1$ (CH₃CH₂O); 1.83 d, 3H, $J(\text{CH}_3, 6) = 1.2$ (5-CH₃); 3.79 s, 3H (CH₃O); 4.08 q, 2H, $J(\text{CH}_2, \text{CH}_3) = 7.1$ (OCH₂CH₃); 7.42 q, 1H, $J(6, \text{CH}_3) = 1.2$ (H-6); 7.79 bs, 1H (H-3). ¹³C NMR (CDCl₃, 125.7 MHz): 9.07 (5-CH₃); 15.26 (CH₃CH₂O); 52.72 (CH₃O); 70.12 (OCH₂CH₃); 107.09 (C-5); 151.93 (C-2); 157.59 (C-6); 165.97 (C-4). HR-MS for C₈H₁₃NO₄Na (M + H + Na)⁺ calcd 210.0742, found 210.0741.

Acknowledgements

The authors gratefully acknowledge the financial support by the Ministry of Education, Youth, and Sports of the Czech Republic (Research projects Z40550506, 2B06065, and LC512) and the Ministry of Health (Grant NR/9138 – 3).

REFERENCES

- [1] C. M. Galmarini, J. R. Mackey, C. Dumontet, *Lancet Oncol.* **2002**, 3(7), 415–424.
- [2] S. Miura, S. Izuta, *Curr. Drug. Target.* **2004**, 5(2), 191–195.
- [3] C. Simons, Q. Wu, T. T. Htar, *Curr. Top. Med. Chem.* **2005**, (13), 1191–1203.
- [4] S. W. Schneller, *Curr. Top. Med. Chem.* **2002**, 2(10), 1087–1092.
- [5] L. S. Jeong, J. A. Lee, *Antivir. Chem. Chemother.* **2004**, 15(5), 235–250.
- [6] A. Holý, *Antivir. Res.* **2006**, 71(2–3), 248–253.
- [7] D. Rejman, M. Masojídková, E. De Clercq, I. Rosenberg, *Nucleosides Nucleotides* **2001**, 20(8), 1497–1522.
- [8] P. Kočalka, R. Pohl, D. Rejman, I. Rosenberg, *Tetrahedron* **2006**, 62, 5763–5774.
- [9] D. Rejman, P. Kočalka, M. Buděšínský, R. Pohl, I. Rosenberg, *Tetrahedron* **2007**, 63(5), 1243–1253.
- [10] K. Yamada, S. Sakata, Y. Yoshimura, *J. Org. Chem.* **1998**, 63, 6891–6899.
- [11] W. Lu, S. Sengupta, J. L. Petersen, N. G. Akhmedov, X. Shi, *J. Org. Chem.* **2007**, 72, 5012–5015.
- [12] B. Y. Michel, P. Strazewski, *Tetrahedron* **2007**, 63, 9836–9841.
- [13] H. M. Abrams, L. Ho, S. H. Chu, *J. Heterocyc. Chem.* **1981**, 18, 947–951.
- [14] M. Tokumi, K. Shigetada, U. Mayuko, *Nucleosides Nucleotides* **1999**, 18(4–5), 661–672.
- [15] T. Keiko, M. Masako, T. Tadakazu, *J. Heterocyc. Chem.* **1997**, 34(2), 669–673.
- [16] G. Shaw, R. N. Warrener, *J. Chem. Soc.* **1958**, 153–156.
- [17] G. Shaw, R. N. Warrener, *J. Chem. Soc.* **1958**, 157–161.
- [18] Y. F. Shealy, C. A. O'Dell, *J. Heterocyc. Chem.* **1976**, 13, 1015–1020.
- [19] P. G. Wyatt, A. S. Anslow, B. A. Coomber, R. P. C. Cousins, D. N. Evans, V. S. Gilbert, D. C. Humber, I. L. Paternoster, S. L. Sollis, D. J. Tapolczay, G. G. Weingarten, *Nucleosides Nucleotides* **1995**, 14, 2039–2049.
- [20] H. Hřebaběcký, M. Masojídková, A. Holý, *Collect. Czech. Chem. Commun.* **2005**, 70, 519–538.
- [21] R. Csuk, Y. von Scholz, *Tetrahedron* **1995**, 51, 7193–7206.
- [22] A. D. Borthwick, D. N. Evans, B. E. Kirk, K. Biggadike, A. M. Exal, P. Youds, S. M. Roberts, D. J. Knight, A. V. Coates, *J. Med. Chem.* **1990**, 33, 179–186.
- [23] M. Bodenteich, V. E. Marquez, J. J. Barchi, W. H. Hallows, B. M. Goldstein, J. S. Driscoll, *J. Org. Chem.* **1993**, 58, 6009–6015.
- [24] F. Hosono, S. Nishiyama, S. Yamamura, *Tetrahedron* **1994**, 50(47), 13335–13346.
- [25] S. Raganathan, K. S. George, *Tetrahedron* **1997**, 53(9), 3347–3362.
- [26] H. Miyabe, S. Kanehira, K. Kume, H. Kandori, T. Naito, *Tetrahedron* **1998**, 54, 5883–5892.
- [27] H. R. Moon, H. O. Kim, M. W. Chun, L. S. Jeong, *J. Org. Chem.* **1999**, 64, 4733–4741.

- [28] P. Wang, B. Gullen, M. G. Newton, Y. C. Cheng, R. F. Shinazi, C. K. Chu, *J. Med. Chem.* **1999**, *42*, 3390–3399.
- [29] S. Bera, T. Mickle, V. Nair, *Nucleosides Nucleotides* **1999**, *18*(11 and 12), 2379–2395.
- [30] H. S. Kim, R. G. Ravi, V. E. Marquez, S. Maddileti, A. K. Wihlborg, D. Erlinge, M. Malmjö, J. L. Boyer, T. K. Harden, K. A. Jacobson, *J. Med. Chem.* **2002**, *45*, 208–218.
- [31] M. I. Nieto, O. Caamaño, F. Fernández, M. Gómez, J. Balzarini, E. DeClercq, *Nucleosides Nucleotides* **2002**, *21*(3), 243–255.
- [32] S. A. Kim, H. M. Lee, J. S. Ryu, H. S. Kim, *Synlett* **2007**, *7*, 1055–1058.
- [33] M. D. Migliore, N. Zonta, C. McGuigan, G. Henson, G. Andrei, R. Snoeck, J. Balzarini, *J. Med. Chem.* **2007**, *50*, 6485–6492.
- [34] Y. F. Shealy, C. A. O'Dell, *J. Heterocyc. Chem.* **1976**, *13*, 1041–1047.
- [35] D. Rejman, S. Kovačková, R. Pohl, M. Dračinský, P. Fiedler, I. Rosenberg, *Tetrahedron* **2009**, *65*(41), 8513–8523.
- [36] J. N. Harvey, *Faraday Discuss.* **2010**, *145*, 487–505.
- [37] R. Ahlrichs, M. Bär, M. Häser, H. Horn, C. Kölmel, *Chem. Phys. Lett.* **1989**, *162*, 165–169.
- [38] J. P. Perdew, K. Burke, M. Ernzerhof, *Phys. Rev. Lett.* **1996**, *77*, 3865–3868.
- [39] A. D. Becke, *Phys. Rev. A* **1988**, *38*, 3098–3100.
- [40] C. T. Lee, W. T. Yang, R. G. Parr, *Phys. Rev. B* **1988**, *37*, 785–789.
- [41] A. D. Becke, *J. Chem. Phys.* **1993**, *98*, 5648–5652.
- [42] P. J. Stephens, F. J. Devlin, C. F. Chabalowski, M. J. Frisch, *J. Phys. Chem.* **1994**, *98*, 11623–11627.
- [43] K. Eichkorn, O. Treutler, H. Öhm, M. Häser, R. Ahlrichs, *Chem. Phys. Lett.* **1995**, *240*, 283–290.
- [44] K. Eichkorn, F. Weigen, O. Treutler, R. Ahlrichs, *Theor. Chim. Acta* **1997**, *97*, 119–124.
- [45] A. Schäfer, H. Horn, R. Ahlrichs, *J. Chem. Phys.* **1992**, *97*, 2571–2577.
- [46] F. Weigend, R. Ahlrichs, *Phys. Chem. Chem. Phys.* **2006**, *7*, 3297–3305.
- [47] A. Klamt, G. Schuurmann, *J. Chem. Soc. -Perkin Trans. 2*, **1993**, 799–805.
- [48] A. Schäfer, A. Klamt, D. Sattel, J. C. W. Lohrenz, F. Eckert, *Phys. Chem. Chem. Phys.* **2000**, *2*, 2187–2193.
- [49] S. Grimme, *J. Comput. Chem.* **2004**, *25*, 1463–1473.
- [50] F. Jensen, *Introduction to Computational Chemistry*. John Wiley & Sons, New York, **1999**.